

Short Communication

## Study on Characteristics and Microstructure of Ni-AlN Thin Coatings Prepared via Different Electrodeposition Techniques

Zhongguo Yang<sup>1</sup>, Shujuan Yi<sup>2,\*</sup>, Yun Wang<sup>1</sup>, Shengxue Zhao<sup>2</sup>, Wang Shi<sup>2</sup>

<sup>1</sup> College of Civil Engineering and Water Conservancy, Heilongjiang Bayi Agricultural University, Daqing 163319, China;

<sup>2</sup> College of Engineering, Heilongjiang Bayi Agricultural University, Daqing 163319, China

\*E-mail: [gyang109@163.com](mailto:gyang109@163.com)

Received: 11 October 2021 / Accepted: 3 December 2021 / Published: 5 January 2022

---

In this work, pulse-current (PC), direct-current (DC), and deposition of ultrasonic-assisted pulse-current (UAPC) were used to produce Ni-AlN thin coatings. X-ray diffractometer (XRD), scanning electron microscopy (SEM), scanning probe microscopy (SPM), Vickers hardness assessment, as well as electrochemical station were used to examine the microhardness, microstructure, and erosion properties of Ni-AlN thin coatings. The coatings based on Ni-AlN, generated using UAPC deposition had a fine compact morphological property. The respective mean grain sizes of the particles of Ni and AlN were about 97.4 and 40.1 nm, according to the SPM data. The thin coatings comprise Ni and AlN phases, according to the XRD data. The thin coatings of Ni-AlN produced using PC, DC and UAPC deposition techniques, respectively, demonstrated optimum microhardness values of 939, 902, and 986 HV when the current density was 4.5 A/dm<sup>2</sup>. When compared to the corrosion resistance of the coatings obtained through UAPC deposition with the other two types of thin coatings, the results showed that the coatings obtained through UAPC deposition manifested the highest value of corrosion resistance.

---

**Keywords:** Electrodeposition; microstructure; Ni-AlN thin coating; corrosion

### 1. INTRODUCTION

As a ceramic material, aluminum nitride is frequently utilized in dielectric materials, optoelectronics, ceramic filters, insulating films, and rural water supply pipes. AlN nanoparticles are frequently added to nickel-based coatings, to improve their quality, such as wear resistance, microhardness, and corrosion resistance [1-5]. Electrodeposition is commonly used to combine various types of ceramic particles with various metals because it is relatively easy to operate and more controllable [6-12]. During the past few years, the successful fabrication of thin metal coatings of many

kinds has been accomplished. Fan *et al.* [13] utilized a Watts bath for the electrodeposition of Ni-P-diamond thin coatings. Hexadecylpyridinium bromide, a cationic surfactant, may efficiently suppress particle aggregation, ensuring that diamond particles are equally dispersed in the nickel matrix. Xia and colleagues [14] employed a jet DC electroplating method for the preparation of Ni-doped TiN composites. Some major process parameters were thoroughly investigated and optimized for their influence on the microstructure characteristics of Ni-doped TiN composite coating. These included the solution stirring speed, TiN nanoparticle concentration as well as current density. Ni-Co-SiC composite thin coatings were fabricated by Ma *et al.* [15], through ultrasound-assisted pulse-current (UAPC) deposition technology. The mean diameter of the grain of Ni and SiC films prepared by UAPC deposition was found to be 69.7 and 28.5 nm. Nanocomposite coatings based on Ni-Al<sub>2</sub>O<sub>3</sub> with different Al<sub>2</sub>O<sub>3</sub> contents were deposited by Majidi *et al.* [16] via pulse electrodeposition method in an improved Watts bath containing Al<sub>2</sub>O<sub>3</sub> nanoparticles. The results show that the quantity and distribution of matrix and co-deposited ceramic particles largely determine the key properties of the film. Various process parameters influence this distribution, including the concentration of ceramic particles in the solution, the composition of the electrolyte, and the implemented current (current density, DC, and PC) [17-20]. Though there are quite a lot of reports focusing on the DC or PC deposition of metals [21-23], there are relatively few reports on the application of UAPC deposition in the preparation of Ni-AlN thin coatings.

As a result, research regarding the fabrication process and characterization of coatings based on Ni-AlN by employing the UAPC deposition technology is required. The novelties of this paper are listed as follows: (1) Three kinds of Ni-AlN coatings were successfully created using three different processes in this research, including DC, PC, and UAPC-deposited thin films. (2) The UAPC deposition process can be used to prepare Ni-AlN thin coatings with good characteristics. (3) The three Ni-AlN coatings that were developed for this study were evaluated in terms of their morphology and mechanical properties. Meanwhile, the coatings' eroding properties were also investigated.

## 2. MATERIALS AND METHODS

The electrodeposition facilities employed in this investigation are represented in Figure 1. High-frequency axial vibration signals (20 kHz) were generated by an ultrasonic generator (UXL-600, Shanghai Youli Science and Technology Development Co., Ltd) and converted into mechanical vibrations, employing a transducer. The ultrasonic generator furnishes a maximum power of 500 W. The plating bath was supported by metallic frames (180×180×110 mm<sup>3</sup>). For filling in the electrolyte, the employed plating bath was made from plastic and bore the dimensions 85×85×70 mm<sup>3</sup>. For DC, PC, and UAPC electrodeposition operations, a power supply, namely pulse plating (SMD-60, Dashun Electroplating Equipment Co., Ltd) was used. Thin coatings based on Ni-AlN (50 μm thick) were deposited on 25×25×6 mm<sup>3</sup> steel substrates, using three different deposition methods: DC, PC, and UAPC. An ultrasonic thickness gauge (TT100, Beijing Taiyu Technology Co., Ltd) was used to determine the thickness of the produced thin layer. In the deposition procedure, steel substrates were used as a cathode.

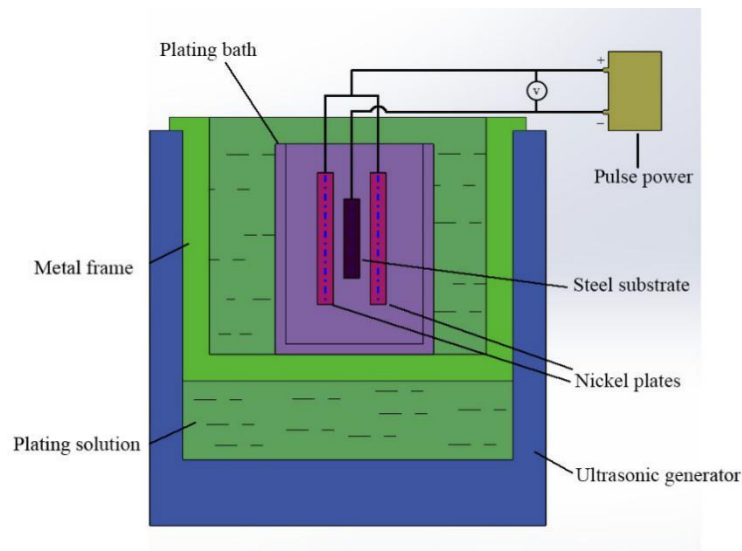


**Figure 1.** Experimental graph for fabricating Ni-AlN thin coatings.

Substrate polishing was carried out before being employed for deposition, and a roughness tester was used to assess the roughness of the surface ( $R_a$ ) for the polished substrate (SV-RT110, Huazhi Instruments and Apparatus Co., Ltd). The surface roughness value after polishing was  $0.15 \mu\text{m}$ . The anode comprised a pair of Ni plates of size  $40 \times 40 \times 5 \text{ mm}^3$ . The solutions and electroplating parameters used to prepare the electrolyte for Ni-Al films are listed in Tables 1 and 2. During the process of electrodeposition, the particles of AlN (30 nm) were added to the electrolyte. Transmission electron microscopy was used to examine the surface of AlN particles produced via deposition (TEM, Tecnai-G2-20-S-Twin, FEI Co., Ltd, Columbia, MD, USA). The TEM pictures representing the particles of AlN are depicted in Figure 2, which illustrates the microscopic nano size, aggregation, and shape regularity of the AlN particles.

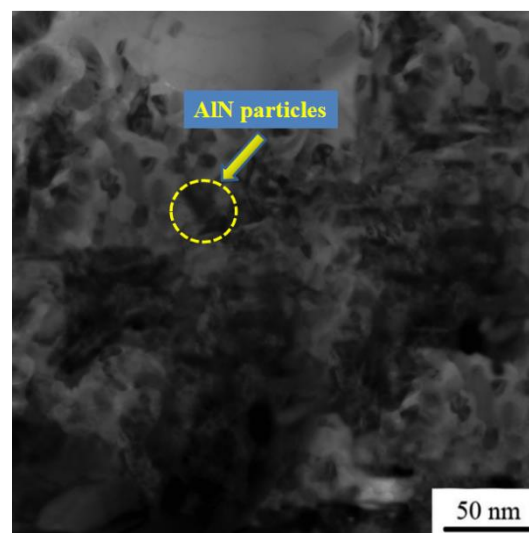


**Figure 2.** TEM photograph for the AlN nanoparticles.

**Table 1.** Electrolyte composition for preparing the Ni–AlN thin coatings.

Compositions	Parameters
NiSO <sub>4</sub>	250 g/L
NiCl <sub>2</sub>	30 g/L
H <sub>3</sub> BO <sub>3</sub>	28 g/L
Cetyltrimethyl ammonium bromide	50 mg/L
AlN nanoparticle	8 g/L
pH	4.8
Temperature	50°C

**Table 2.** Parameters of operating for Ni-AlN thin coating electrodeposition.

Deposition method	DC deposition	PC deposition	UAPC deposition
Current density (A/dm <sup>2</sup> )	3~5	3~5	3~5
Pulsed frequency (Hz)		100	100
Duty cycle		0.6	0.6
Ultrasonic power (W)			250
Electroplating time (min)	60	60	60

The surface morphological attributes of Ni-AlN thin coating obtained *via* deposition were studied using scanning electron microscopy (SEM, JSM-5610LV) equipped with energy dispersive X-ray assessment (EDS, IE-300X, Oxford Semiconductor Co., Ltd). Additionally, the samples were subjected to scanning probe microscopy (SPM, Nanoscope IIIa, Veeco Co., Ltd, Plainview, NY, USA). The phase structural details of the coatings based on Ni-AlN were investigated by carrying out X-ray diffraction analysis using a D/Max-2400 apparatus (Rigaku Co., Ltd, Akishima-shi, Tokyo, Japan) with the radiation of Cu-K $\alpha$  (0.15418 nm). A 401 MVT tester of microhardness (Shanghai Precision Instruments Co., Ltd, Shanghai, PR China) was used to test the Vickers hardness under a 100 gf load for 15 seconds. A CHI 650B electrochemical workstation (Shanghai Huachen Instruments Co., Ltd, Shanghai, PR China) was used to conduct a 30-hour corrosion test of Ni-AlN composite thin coatings at room temperature in an aerated 3.5 wt% solution of NaCl at a scanning rate of 0.05 mV/s. A saturated calomel electrode (SCE) with a lugging capillary was employed to test the electrode potential without IR drops. The electronic analytical balance (BS210S) was employed for the estimation of weight loss.

### 3. RESULTS AND DISCUSSION

#### 3.1 Microstructures of Ni-AlN thin coatings

The SPM photographs for the three thin coatings of Ni-AlN were obtained, and are shown in

Figure 3. By comparison, we discovered that PC-deposited Ni-AlN coatings have a reasonably regular and compact morphology, whereas DC-deposited Ni-AlN coatings have a rough and non-homogeneous structure.

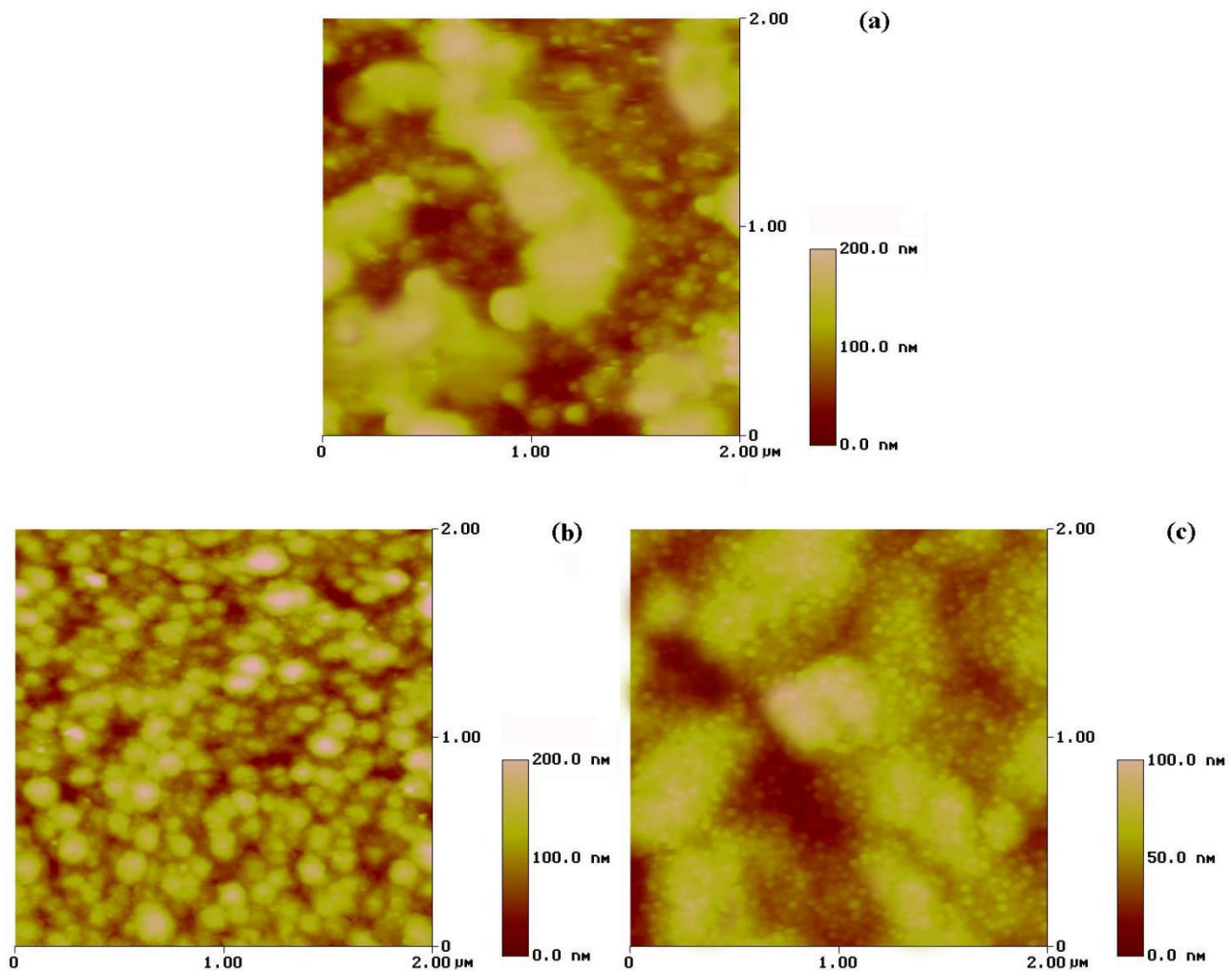
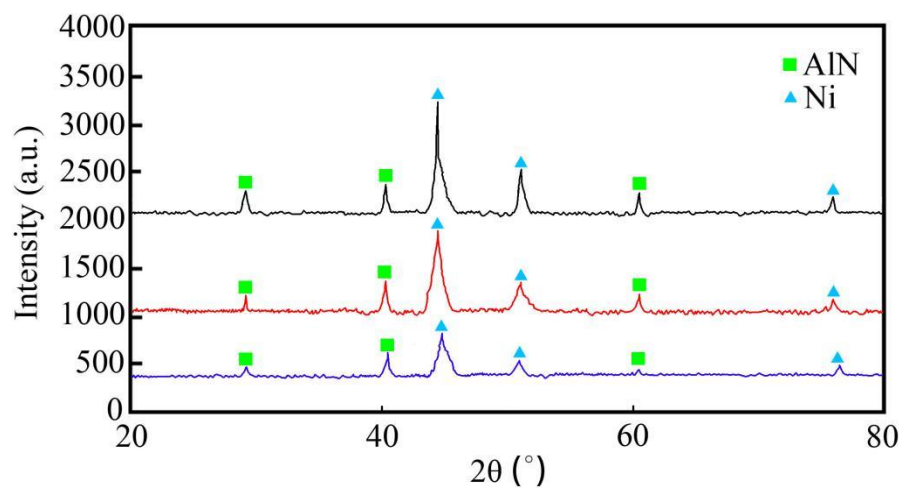


**Figure 3.** Photographs of SPM for Ni-AlN thin coatings deposited through (a) DC (current density  $4\text{A}/\text{dm}^2$ , electroplating time 60 min), (b) PC (current density  $4\text{A}/\text{dm}^2$ , pulsed frequency 100 Hz, duty cycle 0.6, electroplating time 60 min), and (c) UAPC (current density  $4\text{A}/\text{dm}^2$ , pulsed frequency 100 Hz, duty cycle 0.6, ultrasonic power 250 W, electroplating time 60 min) techniques.

The PC technique has the potential to increase the nucleation quantity of Ni grains while restricting their development. Furthermore, the Ni-AlN coating generated via UAPC deposition has a compact and exposed morphological property. The size of the grain of the film is lower in comparison to that of other films, due to the ultrasonic treatment. PC also interferes with Ni crystal development, resulting in bigger crystals that are unable to form smaller nuclei [24]. Ni granules in the thin coating generated via UAPC deposition have a mean diameter of 97.4 nm, while AlN grains have an average

diameter of 40.1 nm. The findings show that among the three deposition methods employed, the morphology of coatings created by UAPC deposition is the best. The morphology of coatings deposited by DC was the poorest. This is in good agreement with the result reported by Wu *et al.* [25].

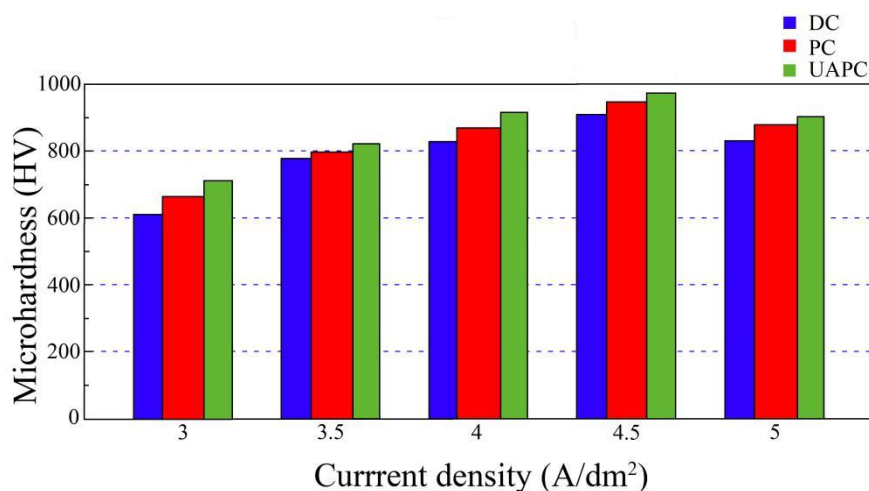
An assessment for the patterns of XRD related to Ni-AlN coatings of the three kinds established the existence of AlN particles. Using a scan step of about  $0.02^\circ$ , the patterns of XRD were obtained from  $20^\circ$  to  $80^\circ$ . The patterns of XRD for the Ni-AlN thin coatings of each of the three types are shown in Figure 4. The coatings are made up of the Ni and AlN phases. The (2 2 0), (2 0 0), and (1 1 1) planes are represented by the peaks of diffraction at  $76.7^\circ$ ,  $52.1^\circ$ , and  $44.6^\circ$  for the grain of Ni, respectively. The peaks of diffraction at  $61.7^\circ$ ,  $42.4^\circ$ , and  $36.6^\circ$  for AlN particles relevant to the (2 2 0), (2 0 0), and (1 1 1) planes, accordingly.



**Figure 4.** Outcomes of XRD for Ni-AlN thin coatings deposited through (a) DC (current density  $4\text{A}/\text{dm}^2$ , electroplating time 60 min), (b) PC (current density  $4\text{A}/\text{dm}^2$ , pulsed frequency 100 Hz, duty cycle 0.6, electroplating time 60 min), and (c) UAPC (current density  $4\text{A}/\text{dm}^2$ , pulsed frequency 100 Hz, duty cycle 0.6, ultrasonic power 250 W, electroplating time 60 min) techniques.

### 3.2 Microhardness for the Ni-AlN thin coatings

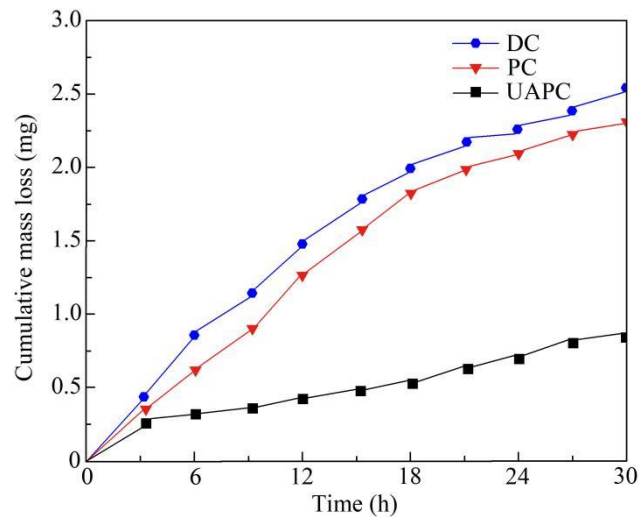
The relationship between the implemented current density and the microhardness of each of the three types of Ni-AlN coatings is depicted in Figure 5. From  $3\text{A}/\text{dm}^2$  to  $5\text{A}/\text{dm}^2$ , the microhardness of thin coatings increases with the upsurge in the implemented current density. The optimum microhardness values for the thin films based on Ni-AlN formed at  $4.5\text{A}/\text{dm}^2$  current density via UAPC, DC, and PC deposition was 902, 939, and 986 HV respectively. The best microhardness values of Ni-AlN coatings were produced through three different deposition processes (DC, PC, and UAPC) are 902, 939, and 986 HV, respectively (upon current density adjustment to  $4.5\text{A}/\text{dm}^2$ ). The dispersion hardening impact generated by AlN particles can help improve the microhardness of thin coatings to some extent. This is due to the strong microhardness of AlN particles, which can improve the performance of Ni-AlN thin coatings. The results are similar to the phenomena described by Aal *et al.* [26].



**Figure 5.** Plots of microhardness against implemented current density employed for Ni-AlN thin coating electrodeposition: DC (current density 4A/dm<sup>2</sup>, electroplating time 60 min), PC (current density 4A/dm<sup>2</sup>, pulsed frequency 100 Hz, duty cycle 0.6, electroplating time 60 min), and UAPC (current density 4A/dm<sup>2</sup>, pulsed frequency 100 Hz, duty cycle 0.6, ultrasonic power 250 W, electroplating time 60 min).

### 3.3 Erosion dynamics of Ni-AlN thin coatings

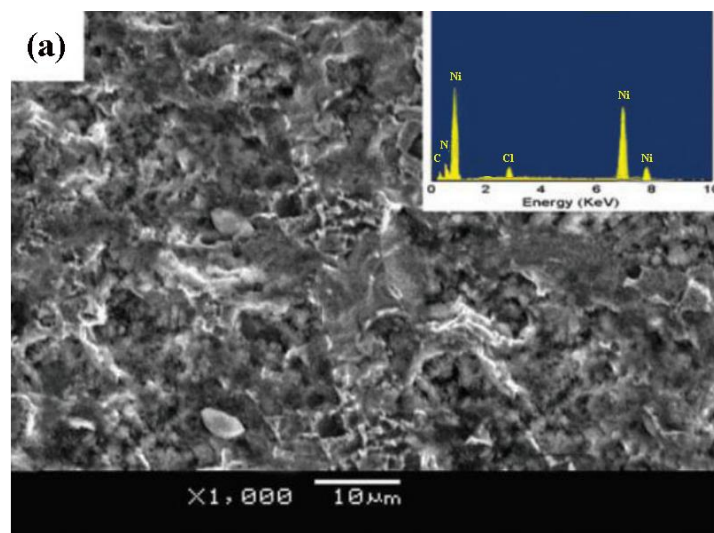
The influence of time upon the weight loss of each of the three kinds of coatings, based on Ni-AlN is depicted in Figure 6. The coatings are subjected to erosion conditions, and the weight loss is monitored every three hours. The eroding process can take up to 30 hrs. The thin coatings of Ni-AlN, created through PC and DC deposition processes have essentially identical corrosion curves, as shown by the results: the curve first increased significantly at the beginning and subsequently altered slowly. The respective mass loss of the coatings generated by PC, DC, and UAPC deposition was 1.95, 2.14, and 0.60 mg during a 21 hrs erosion test. It can be seen that Ni-AlN films created using the UAPC deposition process have greater corrosion resistance than coatings created using the DC or PC deposition methods. This is because the uniform dispersion of particles of AlN within the Ni-AlN film benefits from an appropriate ultrasonic treatment. Furthermore, the incorporation of AlN particles into the coatings improves the coating's compactness and corrosion resistance. This result is practically the same as the experiment reported by Liu *et al.* [27].



**Figure 6.** Curves of weight loss for thin films of Ni-AlN the following corrosion: DC (current density  $4\text{A}/\text{dm}^2$ , electroplating time 60 min), PC (current density  $4\text{A}/\text{dm}^2$ , pulsed frequency 100 Hz, duty cycle 0.6, electroplating time 60 min), and UAPC (current density  $4\text{A}/\text{dm}^2$ , pulsed frequency 100 Hz, duty cycle 0.6, ultrasonic power 250 W, electroplating time 60 min) techniques.

### 3.4 Morphologies of corrosion for the Ni-AlN thin coatings

The SEM photographs of the coatings following 30 hours of corrosion testing are illustrated in Figure 7. On the surface of DC and PC deposited Ni-AlN films, the existence of some huge pores is evident, however, miniscule pits can be seen upon the surface of UAPC deposited Ni-AlN films. As a result, ultrasonic treatment can help the film disperse microscopic particles more effectively. The nanoparticles of AlN contained in the coatings can alter the surface structures. The coating surfaces smooth down and become dense, thereby preventing direct contact between the coating and the solution. As a result, the Ni-AlN coating corrosion resistance has been enhanced. The results are consistent with the investigation explicated by Wang *et al.* [28].



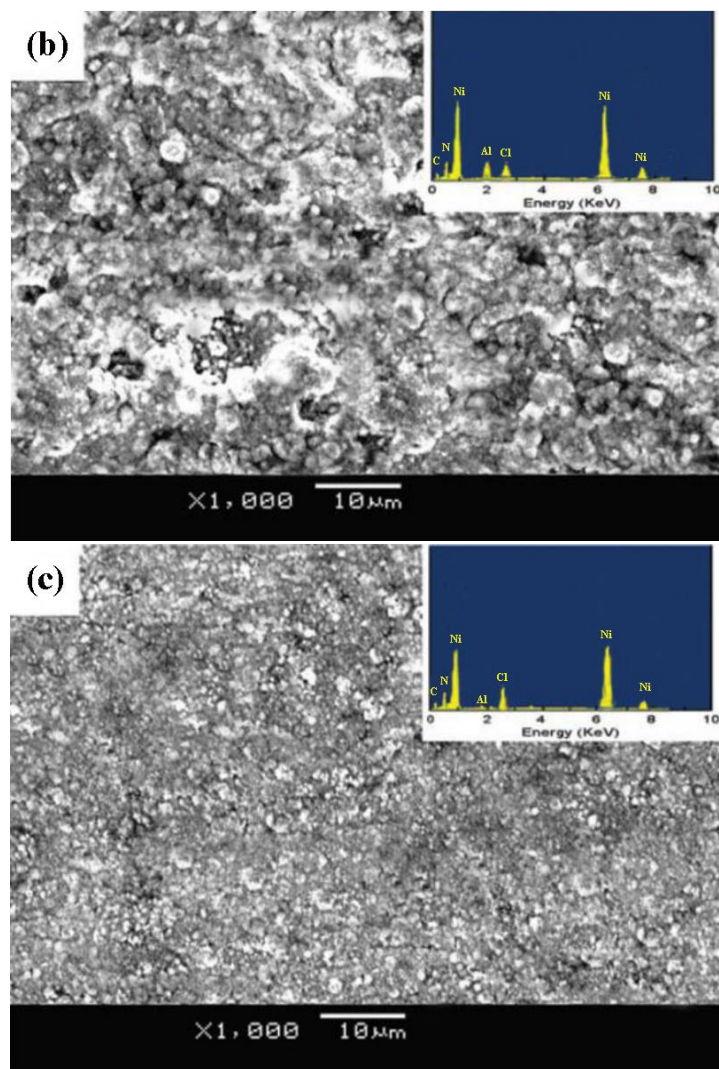


**Figure 7.** SEM photographs of specimens following corrosion assessment: (a) DC (current density  $4\text{A}/\text{dm}^2$ , electroplating time 60 min), (b) PC (current density  $4\text{A}/\text{dm}^2$ , pulsed frequency 100 Hz, duty cycle 0.6, electroplating time 60 min), and (c) UAPC (current density  $4\text{A}/\text{dm}^2$ , pulsed frequency 100 Hz, duty cycle 0.6, ultrasonic power 250 W, electroplating time 60 min) techniques.

### 3.5 Potentiodynamic polarization curves of the Ni-AlN thin coatings

The typical curves of potentiodynamic polarization for three deposited Ni-AlN films produced using the potentiometric polarization approach are shown in Figure 8. Table 3 contains corrosion parameters derived from the potentiodynamic polarization curves. Thin coatings generated by PC-, DC-, and UAPC deposition have respective corrosion potentials of  $-0.468$ ,  $-0.551$ , and  $-0.443$  V vs. SCE. Furthermore, UAPC deposited thin coatings displayed a corrosion current density of  $3.51 \times 10^{-5}$   $\text{A}/\text{cm}^2$ , which was the lowest of all the samples. The phenomenon is consistent with the study reported by Ma *et al.* [29].

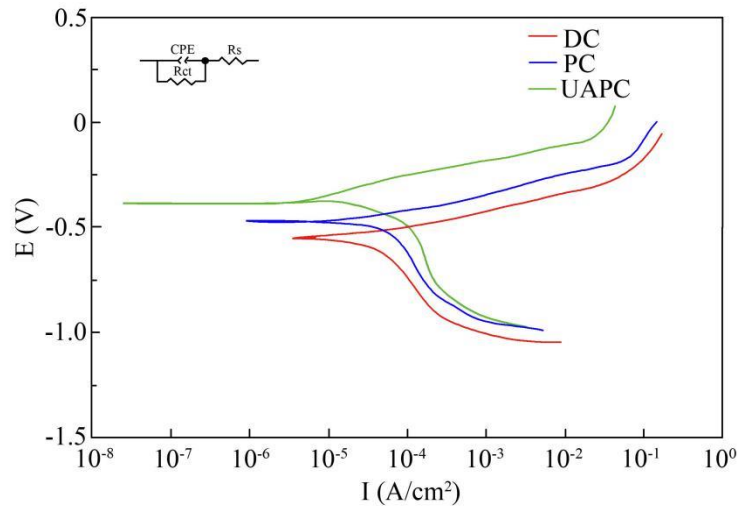


**Figure 8.** Potentiodynamic polarization curves for the thin coatings of Ni-AlN deposited through (a) DC (current density 4A/dm<sup>2</sup>, electroplating time 60 min), (b) PC (current density 4A/dm<sup>2</sup>, pulsed frequency 100 Hz, duty cycle 0.6, electroplating time 60 min), and (c) UAPC (current density 4A/dm<sup>2</sup>, pulsed frequency 100 Hz, duty cycle 0.6, ultrasonic power 250 W, electroplating time 60 min) techniques.

**Table 3.** Electrochemical parameters for the thin coatings of Ni-AlN in a solution of NaCl (3.5 wt%).

Types of coatings	DC-deposited coating	PC-deposited coating	UAPC-deposited coating
$\beta_a$ (V/dec)	0.043	0.021	0.023
$\beta_c$ (V/dec)	0.032	0.031	0.033
$R$ ( $\Omega/\text{cm}^2$ )	2547	3937	6864
$E_{corr}$ (V) vs. SCE	-0.551	-0.468	-0.443
$I$ (A/cm <sup>2</sup> )	$5.46 \times 10^{-5}$	$4.65 \times 10^{-5}$	$3.51 \times 10^{-5}$

#### 4. CONCLUSIONS

(1) The coatings generated via UAPC deposition possessed the most compact and fine morphology, according to SPM data. Ni particles with thin coatings have a mean grain diameter of 97.4 nm, while AlN particles have a mean grain diameter of 40.1 nm. The thin coatings based on Ni-AlN are fabricated out of AlN and Ni phases, according to the XRD data. The (1 1 1 1), (2 0 0), and (2 2 0 0) planes correspond to the peaks of diffraction for AlN particles at 36.6°, 42.4°, and 61.7°, respectively.

(2) The respective microhardness values of PC, DC, and UAPC deposited Ni-AlN thin coatings were 939, 902, and 986 HV when the current density was set to 4.5 A/dm<sup>2</sup>. The dispersion hardening impact generated by AlN particles can help improve the microhardness of thin coatings to some extent.

(3) When comparing the corrosion resistance of the coatings obtained through UAPC deposition

to the other two types of thin coatings, the results showed that the coatings obtained through UAPC deposition manifested the highest value of corrosion resistance. The DC-, PC-, and UAPC-deposited coatings had respective corrosion potentials of -0.551, -0.468, and -0.443 V vs. SCE.

#### ACKNOWLEDGEMENT

This work has been supported by the Heilongjiang Postdoctoral Foundation of China (Granted No. LBH-Z20183), the Heilongjiang Bayi Agricultural University Support Program for San Heng San Zong (Granted Nos. TDJH201803 and TDJH202005), and the Scientific Research Starting Foundation for Returnees and Excellent Scholars (Granted No. XDB201804).

#### References

1. F. Xia, Q. Li, C. Ma and X. Guo, *Ceram. Int.* 46(2) (2020) 2500.
2. T. Jiang, J.G. Munguia-Lopez, S. Flores-Torres, J. Kort-Mascort and J.M. Kinsella, *Appl. Phys. Rev.* 6 (2019) 011310.
3. K. Liu, Y. Li and J. Wang, *Mater. Design.* 105 (2016) 171.
4. M. Nur-E-Alam, M.M. Rahman, M.K. Basher, M. Vasiliev and K. Alameh, *Coatings* 10(3) (2020) 251.
5. G. Li, C. Wang, H. Zhang, M. Zhuang and L. Wang, *Mater. Lett.* 280 (2020) 128598.
6. F. Xia, C. Li, C. Ma, Q. Li and H. Xing, *Appl. Surf. Sci.* 538 (2021) 148139.
7. W. Jiang, L. Shen, M. Qiu, X. Wang, M. Fan and Z. Tian, *J. Alloy. Compd.* 762 (2018) 115.
8. G.C. Efe, S. Zeytin and C. Bindal, *Mater. Design.* 36 (2012) 633.
9. L.J.D. Oliveira, R.P.D.R. Paranhos, R.D.S. Guimarães, G. S. Bobrovnichii and M. Filgueira, *Powder. Metall.* 50(2) (2007) 148.
10. J. Zhang, H.Y. Xu, X.L. Jin, Q.J. Ge and W.Z. Li, *Appl. Catal. A. Gen.* 290(1) (2005) 87.
11. F. Xia, Q. Li, C. Ma, W. Liu and Z. Ma, *Ceram. Int.* 46(6) (2020) 7961.
12. F. Xia, Q. Li, C. Ma, D. Zhao and Z. Ma, *Int. J. Electrochem. Sci.* 15 (2020) 1813.
13. Q. Fan, Y. Gao, Y. Zhao, Q. Yang, L. Guo and L. Jiang, *Mater. Lett.* 215 (2018) 242.
14. F.F. Xia, W.C. Jia, C.Y. Ma, R. Yang, Y. Wang and M. Potts, *Appl. Surf. Sci.* 434 (2018) 228.
15. C. Ma, D. Zhao and Z. Ma, *Ceram. Int.* 46(8) (2020) 12128.
16. H. Majidi, M. Aliofkhazraei, A. Karimzadeh and A. Sabour Rouhaghdam, *B. Mater. Sci.* 39(7) (2016) 1691.
17. M. Shourgeshty, M. Aliofkhazraei and A. Karimzadeh, *Surf. Eng.* 35(2) (2019) 167.
18. S. Mirzamohammadi, H. Khorsand, M. Aliofkhazraei and D.V. Shtansky, *Tribol. Int.* 117 (2018) 68.
19. S. Mirzamohammadi, H. Khorsand and M. Aliofkhazraei, *Surf. Coat. Tech.* 313 (2017) 202.
20. M. Alizadeh and A. Cheshmpish, *Appl. Surf. Sci.* 466 (2019) 433.
21. N. Wasekar, S. Latha, M. Ramakrishna, D. Rao and G. Sundararajan, *Mater. Design.* 112 (2016) 140.
22. R. Sen, S. Das and K. Das, *J. Nanosci. Nanotechno.* 10(12) (2010) 8217.
23. E. Beltowska-Lehman, P. Indyka, A. Bigos, M. Szczerba and M. Kot, *Mater. Des.* 80 (2015) 1-11.
24. C. Ma, W. Yu, M. Jiang and F. Xia, *Ceram. Int.* 44(5) (2018) 5163.
25. Z.H. Wu, W.C. Zhou, F. Luo and D.M. Zhu, *J. Inorg. Mater.* 26(10) (2011) 1063.
26. A.A. Aal, M. Bahgat and M. Radwan, *Surf. Coat. Tech.* 201(6) (2006) 2910.
27. T. Liu, C. Li, Q. Li, L. Li, F. Xia, H. Xing and C. Ma, *Int. J. Electrochem. Sci.* 16 (3) (2021) 151028.
28. H. Wang, W. Yu, H. Liu, Q. Li, F. Xia and C. Ma, *Int. J. Electrochem. Sci.* 16(4) (2021) 210423.

29. C. Ma, D. Zhao, H. Xia, F. Xia, Z. Ma, and T. Williams, *Int. J. Electrochem. Sci.*, 15 (2020) 4015.

© 2022 The Authors. Published by ESG ([www.electrochemsci.org](http://www.electrochemsci.org)). This article is an open access article distributed under the terms and conditions of the Creative Commons Attribution license (<http://creativecommons.org/licenses/by/4.0/>).